Proceedings of the
American Control Conference
San Francisco, California • June 1993

Synthesis Methods for Robust Nonlinear Control

Daniel Bugajski
Systems and Research Center
Honeywell Inc.
3660 Technology Drive
Minneapolis, MN 55418

Dale Enns
Systems and Research Center
Honeywell Inc.
3660 Technology Drive
Minneapolis, MN 55418
and
Aerospace Engineering
University of Minnesota

Allen Tannenbaum
Department of Electrical Engineering
University of Minnesota
Minneapolis, MN 55455

Abstract

In this paper, we will discuss the application of robust control techniques and especially μ-synthesis to the Army's ATB-1000 test fixture. For comparison, two SISO controller designs are also described. The test fixture is pattered after the Apache helicopter's 30 mm gun and has tunable nonlinearities which may be representative not only of the nonlinearities of the gun, but of other mechanical systems as well. The models of the test fixture which were available at the time of the work are also described. The goal in pointing the gun is to reduce dispersions of fired gun rounds on targets. The resulting μ-synthesis design, when connected with a nonlinear simulation, exhibited limit-cycle behavior of unacceptable amplitude. The unacceptable performance is due to the nonlinearities and, in future work, would be improved upon by frequency domain trade-offs during the synthesis step. In particular, we will sketch the use of advanced nonlinear H^∞ techniques for such problems.

1 Introduction

In this paper, we will consider some novel robust control synthesis procedures for nonlinear systems. We will focus our attention on the ATB1000 test fixture at the Picatinny Arsenal in New Jersey which is patterned after the Apache's 30 mm gun.

For proper overall functioning of most of the Army's weapons systems, specific subsystems demand high precision control. For example, a guided munition system may be fitted with laser systems for ranging and/or targeting. Both of the laser subsystems call for accurate pointing control systems. These are in addition to the high performance guidance and control of the munition itself. Tank and gun systems require stabilized platforms from which rapid firing and re-targeting occur. Stabilized platforms are also necessary for antenna systems and video camera systems which are envisioned in future battlefield scenarios. Oftentimes, the accuracy of these control laws is limited by the mechanical system itself, for example, dead zones in gear drives, or friction in bearings.

The Army Research Office has built a laboratory fixture to study control laws for problems that are dominated by "hard" nonlinearities. Example nonlinearities in this group are saturations, static friction effects, and gear backlash. The fixture, the ATB-1000, is patterned after the Apache helicopter gun, and has built-in tunable nonlinearities. It is ideal for studying problems in application of linear and nonlinear control law designs.

This paper offers three potential linear control designs for the ATB-1000. Section 2 briefly discusses the objectives for the design, and Section 3 describes the models available for design and analysis. Section 4 discusses the three different designs, and Section 5 contains some nonlinear simulation and linear analyses for one of the designs. Finally in Section 6, we outline an advanced design technique that we plan to apply in the future.

2 System Requirements

The ATB-1000 is a test fixture patterned after the Apache's 30 mm gun. The basic goal for this weapon is to reduce dispersion of its rounds on targets. So the objective for the ATB-1000 is to minimize the barrel pointing angle deviation from a commanded value in the presence of platform motion (simulated with disk motion), gun firing-induced transients (simulated with a solenoid), and mechanism nonlinearities (simulated with adjustable backlash and friction). The laboratory fixture (see Figure 1) is outfitted with a laser arm to accurately measure the barrel tip position and hence experimentally determine performance. There are also disturbance levels and ranges of parametric nonlinearity adjustments that are part of the requirements.

3 Models

In practice, the development of a successful control system design is highly dependent on obtaining representative models of the system to be controlled. The models are a direct input to the control law synthesis and analysis steps in the development process. Models and modeling data come in many different forms, and different types of models are used for different purposes. Two distinct models of ATB-1000 test fixture were examined as part of this preliminary control design effort. These two models will be described and compared in this section. Some discrepancies between these two models have been identified and it will be necessary to resolve them for future studies.

During the summer of 1991, modeling data was received and analyzed from the Army Research Office. The modeling material consisted of MatrixX block diagrams, tables containing definitions, scale factors, sign conventions, units, signal size information, and linear models for the truncated finite element model of the barrel (with 8 states) and a 27th order identification model. This section will refer to an analytical model and an identification model. The analytical model is based on the block diagrams, tabular data, first principles of dynamics, and includes four relay-type nonlinearities and two deadband-type nonlinearities. The identification model is a linear model whose inputs and outputs are a subset of those in the analytical model.

The MatrixX block diagrams and the tabular data were used to generate a linear model and a nonlinear simulation using Honeywell computer tools. The linear model treats the deadband as a unity operator which neglects backlash, and the relay as a zero operator which neglects friction. The linear model was then examined in terms of its poles, transfer function zeros for certain inputs and outputs, and time and frequency responses. There are degrees-of-freedom for the disk translation and rotation in a plane, motor rotation, inertia wheel rotation, laser arm motor rotation, laser arm rotation, and three elastic degrees of freedom for the gun barrel (simulated with a rod attached to the inertia wheel).

The linear open loop model consists of two physical systems: the disk, inertia wheel, and rod system, and the laser arm system. There is a motor associated with each system. There are five pairs of open loop poles at the origin (because friction is neglected) associated with the rigid body degrees-of-freedom. There are two pairs of complex poles associated with the compliances in both systems, and there are three pairs of complex poles associated with the gun barrel resonances with small damping ratios.

The plant transfer function between the control motor torque and the barrel pointing angle can be regarded as a double integrator (at frequencies below 10 rad/sec) with disturbances (from disk motion) and some high frequency elastic modes. The nonlinear simulation was executed with different test inputs to assess its behavior. An identification (ID) model was obtained in a state space format with seven outputs, one input, and 27 states. The outputs are torque motor resolver, backlash resolver, disk velocity, quadcell output, strain gauge #1, strain gauge #2, and torque motor tachometer, the input is the control motor torque, and the 27 states are not physically defined but the linear ID model fits the data from the identification experiments. This model was compared to the analytical model in terms of poles, frequency response, and time histories.

The ID model shows more open loop damping e.g. ζ_{ID}=0.07 versus $\zeta_{analytic}$=0.01 for the first elastic mode (near 31 rad/sec) and ζ_{ID}=0.15 versus $\zeta_{analytic}$=0.084 for the shaft compliance mode (near 55 rad/sec) between torque motor and inertia wheel. The low frequency behavior of the ID model shows a slope of -1 on a Bode gain plot versus the slope of -2 in the analytical model, because friction is present in the identification experiment, but neglected in analytical model. In addition, the low frequency accuracy of the ID model is limited by the length of time used for the identification experiment. Thus the ID model is not close to the analytical model for frequencies below 10 rad/sec. Except for the poles and low frequency asymptote, the ID and analytical models agree for torque motor resolver, backlash resolver, and torque motor tachometer outputs. On the other hand, the ID and analytical models for strain gauge #2 show 180 deg phase discrepancies, and the the quadcell output does not show close agreement at any frequency.

For future design work, it will be necessary to resolve these discrepancies before closed loop testing can be performed. The ID model was utilized (despite these discrepancies) for demonstration of the μ-synthesis design methodology. Actually a balanced realization of the ID model was truncated to twelve states for the μ-synthesis design. The analytical model was utilized to develop alternate control laws with classical approaches. One of these classical alternates uses motor tachometer feedback, and the other has lead and notch compensation of the inertia wheel position. The next section discusses each of these three designs.

4 Control Law Design

In this section a preliminary design effort for the ATB-1000 test fixture will be described in detail. The design is incomplete, but adequately serves as a starting point for future work. To limit the scope of the preliminary effort, the "hard" nonlinearities were neglected for the control synthesis. However closed loop simulations were carried out where the nonlinearities were included. These preliminary simulations showed that the nonlinearities are significant and it will be necessary to include them in future designs. In this preliminary look at control law design, three design approaches were considered. Two approaches were SISO and one was multivariable μ-synthesis. The SISO designs are of interest because they correspond to minimal sensor requirements. The μ-synthesis approach is of interest because the nonlinearities are accounted for by treating them as bounded operators.

The control problem is to point the gun barrel in the face of disturbances. For the demonstration design presented here, the pointing was quantified in terms of the quadcell output and only the solenoid disturbance was included in the design objective. Model uncertainty was incorporated with a multiplicative perturbation at the torque motor location. Sensor noise was also included in the formal μ-synthesis problem statement. More detailed designs would incorporate frequency domain weighting transfer functions, which act as linear bounds for the effects of the six system nonlinearities. Requirements would also be defined and incorporated for actuator activity and physical limitations.

It was necessary to append a solenoid disturbance input (which simulates gun firing) to the ID model. This was done by selecting a constant gain matrix from the frequency response of the analytical model near the first elastic mode frequency. This is an approximation used for expediency during this preliminary design. In a more detailed design effort, the effect of the disturbance input on the equations of motion would be included more carefully into the state-space matrices for the interconnection structure used for μ-synthesis.

It is worth noting that the gun stabilization fixture is similar to a particular elastic structure control problem which has received a large amount of attention in the control and modeling literature. In addition, experimental studies have been performed at various laboratories [7, 4]. The problem is that of rotating disks (at least two) that are connected with rods that are elastic in torsion. These studies motivated the first design.

Colocated SISO Design One of the SISO designs was for colocated feedback between the torque motor resolver and the motor torque. This choice was motivated by the knowledge that under certain assumptions regarding a lower bound for inherent structural damping, and sufficiently high bandwidth sensors, computers, and actuators, such a mechanical system can be robustly stabilized with colocated sensors and actuators even in

the presence of some significant nonlinearities. When the sensor and actuator are not colocated, robust stabilization is, in general, more difficult to achieve due to limitations imposed by non-minimum phase aspects. [11, 12, 1]

The reduced order ID model was utilized to determine the feedback compensation. Recall that the transfer function has a $1/s$ shape below 10 rad/sec in the case of the ID model. Thus a pure gain can be selected to set the unit loop gain crossover at 10 rad/sec as a preliminary design choice. Higher frequency resonances are stabilized because of the colocation and the assumptions about inherent damping, sensors, and actuators. A higher crossover could be considered but this would require more accurate modeling of even higher frequency elastic behavior and tighter requirements on sensors and actuators. A pure gain feedback between motor position and motor torque would not be stabilizing if connected to the analytical model because it has a $1/s^2$ shape below 10 rad/sec as discussed above.

Noncolocated SISO Design The other SISO design was developed with the analytical model for noncolocated feedback between the inertia wheel encoder and motor torque. In this case a lead compensation element was employed to create a unit loop gain crossover at 10 rad/sec. In this case, some of the higher frequency resonances are destabilized by the noncolocated feedback. To prevent this destabilization, notch filters were included for the first elastic mode and the compliant mode between the motor and inertia wheel. This design approach is of interest (as compared to the colocated design) because the colocated motor position is not as closely related to the pointing angle as is the inertia wheel. This design also has value as a further comparison against the μ-synthesis design.

Mu-Synthesis Design The μ-synthesis design approach is multivariable and is cast in terms of the interconnection structure shown in Figure 1. There is a multiplicative perturbation at the torque motor location represented by Δ and the input v_1 and output z_1. There is a performance output called e_{quad} which is the quadcell output passed through a weighting function. The external inputs are sensor noise and the solenoid disturbance. There is also the torque motor input and the seven sensors to close the feedback loop with the compensator K.

The interconnection structure includes weighting transfer functions for uncertainty bounds, performance requirements, and disturbances. The uncertainty was modeled as a multiplicative perturbation and was bounded with a third order Butterworth filter having break frequencies at 20 and 300 rad/sec and a high frequency gain of 675. This can be interpreted as 20% model error below 20 rad/sec and 67,500% model error above 300 rad/sec. The pointing requirement is included by weighting the quadcell output with a low pass transfer function $360(s+10)/(s^2+84s+60^2)$. This has unit steady-state gain, so outputs of less than 1 volt would be acceptable. The seven sensor noises are weighted with the constant value of 0.01, so this corresponds to either volts or counts depending on the sensor. Finally, the solenoid disturbance is weighted with a low pass transfer function $0.3/(s+10)$, so inputs of 0.03 volts are expected. The weightings were not carefully related to the hardware in this preliminary design demonstration. This relationship should be more carefully addressed to better account for known hardware characteristics. In particular a weighting for the disturbance would take into account the duty cycle of the solenoid. Additional inputs and outputs as well as weightings could be utilized to represent the nonlinearities which have not been accounted for in the preliminary design.

The state space solution to the H^∞ control synthesis problem was used to find a feedback compensator K. This compensator has as many states (18) as the interconnection structure and it was possible to reduce the compensator order by residualization to 16 states. The closed loop transfer function is denoted by M and connects the inputs: v_1, solenoid, and sensor noise to the outputs: z_1, and quadcell.

The next step in the μ-synthesis design was to introduce D-scales to properly account for the model uncertainty and performance variable response to external inputs. A constant D-scale=3 was employed because a dynamic D-scale was not deemed necessary in this preliminary design. The D-scale was incorporated by multiplying z_1 by 3 and dividing v_1 by 3 (i.e., DMD^{-1}) and a new interconnection structure P was established. The H^∞ problem was then re-solved for the compensator K and the iterations were terminated. Detailed analyses of this compensator appear in the following section.

5 Analyses

The μ-synthesis results are graphed in Figure 2. There are five plots of Bode magnitude versus frequency. The top curve is relatively flat because it is the maximum singular value of the closed loop interconnection structure ($\bar{\sigma}[M]$), and H^∞ optimization makes its peak value as small as possible. The next curve down is the structured singular value, $\mu[M]$, and is necessarily less than or equal to the upper curve, since $\bar{\sigma}[M]$ is a theoretical upper bound for $\mu[M]$. There is a low frequency difference between the structured and maximum singular values, which indicates that performance improvements are possible by further D-K iteration and frequency dependent D-scales.

The next two curves in Figure 2 correspond to robust stability and nominal performance. Theoretically these curves are less than or equal to the structured singular value and this is consistent with the numerical results. The robust stability curve is relative to to the defined multiplicative perturbation, and dominates $\mu[M]$ at higher frequencies. The robust stability curve can be further interpreted as the weighted complementary sensitivity, where the weighting is the bound for the multiplicative perturbation. The nominal performance curve is the maximum singular value of the transfer function matrix between the weighted quadcell and the external inputs including the weighted solenoid disturbance and sensor noise. This curve dominates $\mu[M]$ at low frequencies and can be further interpreted as the weighted sensitivity. The lowest curve in the figure corresponds to the weighted quadcell response due to sensor noise. This is more than an order of magnitude less than $\mu[M]$, so the quadcell/sensor noise path does not have much influence on the optimal design.

Further analyses of the μ-synthesis design were carried out to assess closed loop poles, input and output loop properties, and time response to solenoid disturbances. The closed loop poles indicated closed loop stability and damping improvements for the first elastic mode ($\zeta_{CL} = 0.12$ versus $\zeta_{OL} = 0.08$) and compliant mode ($\zeta_{CL} = 0.21$ versus $\zeta_{OL} = 0.14$). Gain and phase margins for the SISO loop transfer function at the torque motor actuator location were evaluated. The lowest frequency unit gain crossover occurs at 5.8 rad/sec with a phase margin of 81 degrees. The phase margins surrounding the first elastic

mode frequency are larger than 43 degrees. All gain margins are larger than 7 db. These are considered good margins with respect to model uncertainty at the actuator location.

The linear closed loop system was simulated with the disturbance model used for the μ-synthesis design. This disturbance model is a constant gain matrix between the solenoid and the measurements including the quadcell output. Thus this model is only accurate near the first elastic mode frequency and is not accurate at low or high frequencies. The disturbance input was a 10 Hz sequence of 10 msec, 1 volt pulses. (See Figure 3a.) The quadcell output response is dominated by the the compliant mode because the pulse frequency is close in proximity to the compliant mode frequency. The quadcell output during the 10 msec solenoid firing is not accurate, so disregarding these portions of the response, the quadcell output shows a residual oscillation near the compliant mode frequency with less than 3 volts peak-to-peak. (See Figure 3b.) This is not considered satisfactory performance and the interconnection structure should be further refined to improve the performance by making better tradeoffs with the weighting functions.

6 Nonlinear H^∞

In this section, we will consider new approaches to design using nonlinear generalizations of H^∞ theory which should give bounds for control limitations in the presence of noninvertible nonlinearities such as those present in the ATB-1000. To fix ideas about how such a procedure would go, let us consider the simple sensitivity minimization problem form a nonlinear SISO plant P and weighting filter W. (See [10] for all the necessary assumptions and the precise definitions.)

We consider the problem of finding

$$\mu_\delta := \inf_C \sup_{\|v\| \le \delta} \|[(I + P \circ C)^{-1} \circ W]v\|,$$

where we assume all the operators involved are admissible [10]. Thus we are looking at a worst case disturbance attenuation problem where the energy of the signals v is required to be bounded by some pre-specified level δ. (In the linear case, since everything scales, we can always without loss of generality take $\delta = 1$. For nonlinear systems, we must specify the energy bound *a priori*.) Under the proper assumptions [8, 9, 10], one sees that this problem is equivalent to the problem of finding

$$\mu_\delta = \inf_{q \in C_l} \sup_{\|v\| \le \delta} \|(W - P \circ q)v\|,$$

where C_l denotes the space of causal, analytic operators (see the above references). (All the input/output operators we consider here will be time-invariant as well.)

One can give an iterative procedure for approximating a solution to such a problem. Briefly, the idea is that we write

$$\begin{aligned} W &= W_1 + W_2 + \cdots, \\ P &= P_1 + P_2 + \cdots, \\ q &= q_1 + q_2 + \cdots, \end{aligned}$$

where W_j, P_j, q_j are homogeneous polynomials of degree j. Notice that

$$\mu_\delta = \delta \inf_{q_1 \in H^\infty} \|W_1 - P_1 q_1\| + O(\delta^2),$$

where the latter norm is the operator norm (i.e., H^∞ norm). From H^∞ theory, we can find an optimal (linear, causal, time-invariant) $q_{1,opt} \in H^\infty$ such that

$$\mu_\delta = \delta \|W_1 - P_1 q_{1,opt}\| + O(\delta^2).$$

Now the iterative procedure of [10] gives a way of giving higher order corrections to this linearization. Let us illustrate this now with the second order correction. Indeed, having fixed now the linear part $q_{1,opt}$ of q in the last equation, we note that

$$W(v) - P(q(v)) - (W_1 - P_1 q_{1,opt})(v) =$$

$$W_2(v) - P_2(q_{1,opt}(v)) - P_1 q_2(v) + \text{higher order terms.}$$

Regarding W_2, P_2, q_2 as linear operators on $H^2 \otimes H^2 \cong H^2(D^2, \mathbf{C})$, we see that

$$\sup_{\|v\| \le \delta} \|(W - P \circ q)(v) - (W_1 - P_1 q_{1,opt})v\| \le \delta^2 \|\hat{W}_2 - P_1 q_2\| + O(\delta^3),$$

where the "weight"

$$\hat{W}_2 := W_2 - P_2(q_1 \otimes q_1).$$

We can now use the methods of [10] to pick an optimal admissible $q_{2,opt}$, and so on.

In short, instead of simply designing a linear compensator for a linearization of the given nonlinear system, this methodology allows one to explicitly take into account the higher order terms of the nonlinear plant, and therefore increase the ball of operation for the nonlinear controller. Of course, for a realistic design for the ATB-1000 such a procedure would nave to be applied to the full standard H^∞ problem.

Acnowledgement: This work was supported in part by grants from the National Science Foundation DMS-8811084 and ECS-9122106, by the Air Force Office of Scientific Research AFOSR-90-0024, and by the Army Research Office DAAL03-91-G-0019.

References

[1] G.J. Balas, "Robust Control of Flexible Structures: Theory and Experiments," Ph. D. Dissertation, California Institute of Technonlogy, 1990.

[2] J. Ball and J. W. Helton, "H^∞ control for nonlinear plants: connections with differential games," Proc. of the 28-th CDC, Tampa, Florida, December 1989, pp. 956–962.

[3] J. Ball and J. W. Helton, "Nonlinear H^∞ control theory for stable plants," Technical Report, Department of Mathematics, University of California at San Diego, 1990.

[4] R.H. Cannon and D.E. Rosenthal, "Experiments in control of flexible structures with noncolocated sensors and actuators," *Journal of Guidance Control and Dynamics* **7**, No. 5, p. 546, Sept.-Oct., 1984.

[5] J. C. Doyle, "Analysis of feedback systems with structured uncertainties," *IEE Proc.* **129** (1982), pp. 242–250.

[6] J. C. Doyle, B. Francis, and A. Tannenbaum, *Feedback Control Theory*, McMillan, New York, 1991.

[7] D. Enns, "Model reduction for control system design", Ph. D. Dissertation, Dept. of Aeronautics and Astronautics, Stanford University, 1984.

[8] D. Enns, C. Foias, T. Georgiou, M. Jackson, B. Schipper, and A. Tannenbaum, "On the nonlinear mixed sensitivity problem," Proc. of 28-th IEEE Conference on Decision and Control, Tampa, Florida, December 1989, pp. 2673–2678.

[9] C. Foias and A. Tannenbaum, "Weighted optimization theory for nonlinear systems," *SIAM J. on Control and Optimization* **27** (1989), pp. 842–860.

[10] C. Foias, C. Gu, and A. Tannenbaum, "Nonlinear H^∞ optimization: a causal power series approach," submitted for publication to *SIAM J. on Control and Opt.*

[11] C.S. Greene and G. Stein, "Inherent damping, solvability conditions, and solutions for structural vibration control," Proc. of 1979 IEEE Conference on Decision and Control, December 1979.

[12] D.E. Rosenthal, "Experiments in control of flexible structure with uncertain parameters," Ph. D. Dissertation, Dept. of Aeronautics and Astronautics, Stanford University, 1984.

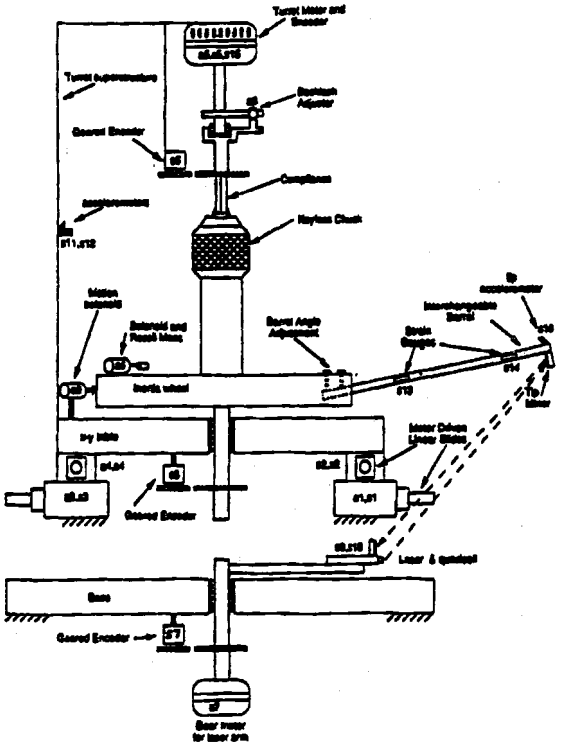

Schematic of ATB-1000 test fixture.

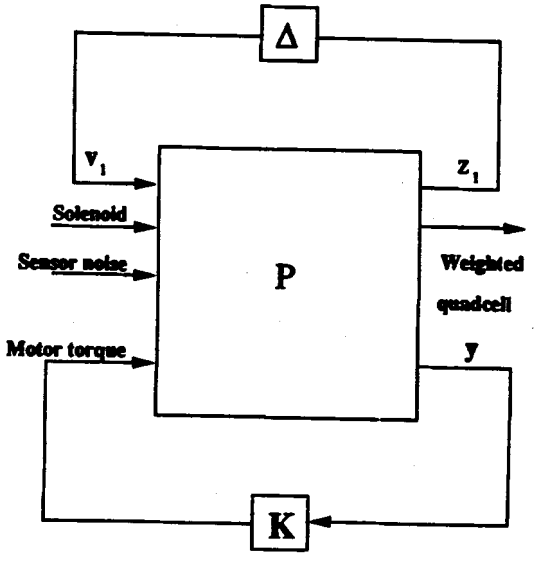

Figure 1. Block diagram of interconnection structure.

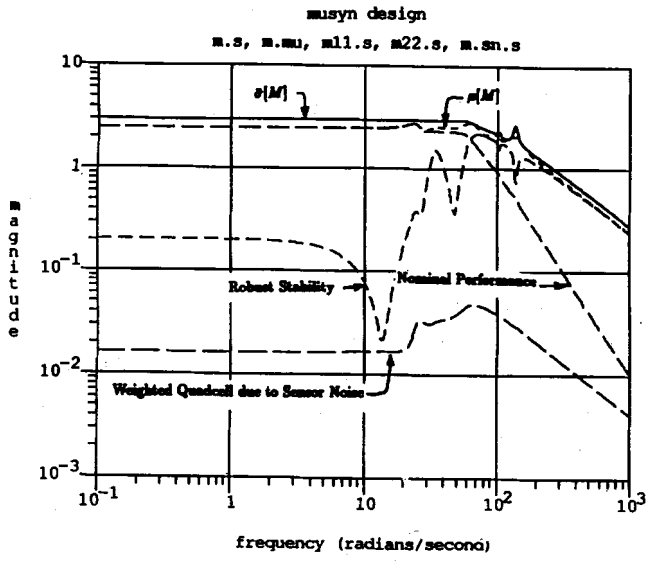

Figure 2. Graphical summary of mu-synthesis design.

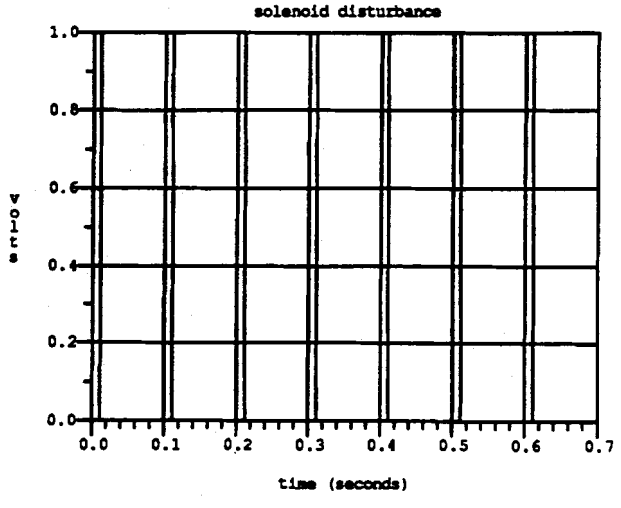

a)

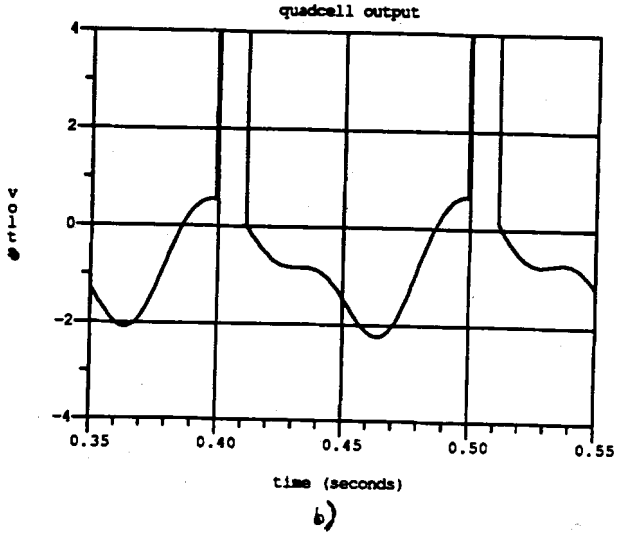

b)

Figure 3. Time histories using mu-synthesis design.